EAST EUROPEAN JOURNAL OF PHYSICS. 3. 310-318 (2026)
DOI:10.26565/2312-4334-2026-3-27 ISSN 2312-4334

RADIATION-INDUCED MODIFICATION OF III–V AND II–VI QUANTUM HETEROSTRUCTURES UNDER HIGH-ENERGY X-RAY, GAMMA-RAY, AND ELECTRON IRRADIATION

Mardonbek Kh. Nasirov[1,2]*, Dilmuhammad X. Tolaboyev[1], Tokhirbek I. Rakhmonov[1], Khusanboy M. Sulaymonov[1], Sherzod Sh. Abdullayev[1], Abdusattor O. Umarov[1], Ixtiyor M. Tursunov[1]

[1]*Fergana State Technical University, Fergana, Uzbekistan*
[2]*Fergana State University, Fergana, Uzbekistan*
**Corresponding Author e-mail: nasirovmardonbek92@gmail.com*

Received April 2, 2026; revised May 15, 2026; in final form June 17; accepted July 6, 2026

Low-dimensional III–V and II–VI quantum heterostructures are important active media for optoelectronic devices operating under radiation environments. In this work, the effects of high-energy X-ray, gamma-ray, and electron irradiation on excitonic recombination and exciton–phonon interaction were investigated in GaAs/AlGaAs and ZnTe/CdZnTe-based quantum heterostructures using low-temperature photoluminescence spectroscopy. The spectra showed pronounced excitonic emission bands accompanied by longitudinal optical phonon replicas, indicating phonon-assisted recombination processes. After irradiation, a substantial reduction in photoluminescence intensity was observed, which was attributed to the formation of radiation-induced non-radiative recombination centers. In ZnTe/CdZnTe structures, electron irradiation produced a slight blue shift (approximately 0.7 meV) of the quantum-well emission, whereas X-ray irradiation resulted in a small red shift (approximately 0.6 meV), suggesting irradiation-dependent modification of exciton localization and defect-related potential fluctuations. A semi-quantitative analysis based on integrated PL intensity ratios, an effective non-radiative recombination parameter, and the Huang–Rhys factor ($S \approx 1–2$) was performed to correlate PL quenching, spectral shifts, and LO-phonon replicas with radiation-induced defect formation. The relative changes in excitonic, impurity-related, and phonon-assisted emission bands indicate a redistribution of radiative and non-radiative recombination channels after irradiation. A phenomenological interpretation based on radiative and non-radiative recombination rates and the Huang–Rhys description of LO-phonon replicas was used to discuss the observed spectral changes. The results provide a comparative experimental assessment of irradiation-induced modifications in III–V and II–VI quantum heterostructures and may be useful for evaluating the radiation tolerance of semiconductor optoelectronic structures.

Keywords: *Radiation-induced defects; Quantum heterostructures; Photoluminescence spectroscopy; Exciton–phonon interaction; LO-phonon replicas; Non-radiative recombination; GaAs/AlGaAs quantum wells; ZnTe/CdZnTe quantum wells*

INTRODUCTION

The interaction of high-energy radiation with semiconductor quantum heterostructures is of fundamental and practical importance for the development of radiation-tolerant optoelectronic devices. Low-dimensional III–V and II–VI quantum heterostructures, including GaAs/AlGaAs and ZnTe/CdZnTe systems, are widely used in lasers, optical modulators, and field-effect transistors because of their tunable electronic and optical properties. In these structures, quantum confinement strongly influences excitonic recombination, impurity-related emission, and phonon-assisted luminescence processes. Recent electro-optical studies of GaAs/AlGaAs multiple quantum wells have shown that their photoluminescence spectra are highly sensitive to quantum confinement and external conditions [1]. Similar excitonic spectral features in related semiconductor structures have also been interpreted in terms of surface radiative modes and longitudinal excitons, thereby emphasizing the complex nature of exciton–polariton luminescence in such systems [2]. ZnTe-based heterostructures are particularly attractive for visible-range optoelectronic applications because they exhibit pronounced excitonic emission and are highly sensitive to structural defects, localization effects, and external perturbations.

Despite extensive research on radiation effects in semiconductors, the microscopic mechanisms governing exciton–phonon coupling in irradiated ZnTe quantum structures remain insufficiently understood. High-energy electron and X-ray irradiation induce defect states that act as non-radiative recombination centers and exciton localization sites, thereby modifying photoluminescence spectra and the relative intensities of excitonic and impurity-related transitions. Recent reviews of irradiated GaAs have likewise shown that radiation-induced point defects and defect complexes play a key role in the formation of non-radiative recombination channels and in the degradation of optical properties [3]. Similar quenching phenomena associated with defect-related non-radiative recombination have been reported in Cd-based semiconductor films under external perturbations such as temperature and infrared excitation [4]. The complex interplay between radiation-induced defects, exciton localization, and phonon-assisted recombination is crucial for understanding and controlling the optical response of these heterostructures under irradiation.

In this study, we investigate the effects of high-energy electron and X-ray irradiation on the low-temperature photoluminescence of ZnTe-based quantum heterostructures. Special attention is paid to longitudinal optical (LO) phonon

Cite as: M.Kh. Nasirov, D.X. Tolaboyev, T.I. Rakhmonov, Kh.M. Sulaymonov, S.Sh. Abdullayev, A.O. Umarov, I.M. Tursunov, East Eur. J. Phys. 3, 310 (2026), https://doi.org/10.26565/2312-4334-2026-3-27

replicas and impurity-related excitonic transitions, which provide insights into the restructuring of luminescence channels induced by radiation. In addition, the role of interband transitions and band structure modifications in determining optical response has been widely discussed in semiconductor systems [5,6]. In this work, the effects of high-energy X-ray, γ-ray, and electron irradiation on the low-temperature photoluminescence response of III–V and II–VI quantum heterostructures are examined with particular attention to excitonic recombination, impurity-related emission, and LO-phonon-assisted spectral features. The study combines experimental PL observations with a phenomenological interpretation based on the competition between radiative and non-radiative recombination channels and the Huang–Rhys description of exciton–phonon coupling. Rather than introducing a new fundamental mechanism, the present work aims to provide a comparative assessment of how different irradiation conditions modify excitonic, defect-related, and phonon-assisted luminescence channels in GaAs/AlGaAs and ZnTe/CdZnTe-based quantum heterostructures. This analysis is intended to clarify the relative sensitivity of different emission bands to irradiation-induced defect formation and to support the evaluation of radiation tolerance in low-dimensional semiconductor structures.

THEORETICAL CONSIDERATIONS

To interpret the observed changes in photoluminescence under irradiation, we employ a phenomenological model that accounts for exciton recombination, radiation-induced non-radiative centers, and exciton–phonon interactions. To describe these coupled processes in a compact form, the total Hamiltonian of the system can be written as

$$H = H_{ex} + H_{ph} + \mathrm{H}_{\text{ex-ph}}, \tag{1}$$

where H_{ex} describes the excitonic subsystem, H_{ph} corresponds to the phonon field, and $H_{\text{ex-ph}}$ represents the exciton–phonon interaction.

Equation (1) defines the general theoretical basis of the model by separating the excitonic, phononic, and interaction contributions to the optical response. For longitudinal optical (LO) phonons, the interaction can be written in the Fröhlich-type form

$$H_{\text{ex-ph}} = \Sigma_q M_q \left(a_q + a_{-}q^{\dagger}\right) X^{\dagger} X, \tag{2}$$

where M_q is the exciton–phonon coupling matrix element, $a_q^{\dagger}$ and a_q are the phonon creation and annihilation operators, and $X^{\dagger}X$ denotes the exciton occupation operator.

Equation (2) explicitly describes the coupling between excitons and LO phonons and serves as the basis for interpreting the phonon-assisted features observed in the PL spectra. This interaction explains the appearance of LO-phonon replicas in the photoluminescence spectra. Such phonon-assisted relaxation channels are characteristic of CdTe/ZnTe quantum well systems, in which LO-phonon emission plays a central role in exciton energy relaxation [7]. The theoretical description of optical absorption processes in semiconductors often relies on interband and intraband transition mechanisms, accounting for band mixing and temperature-dependent effects [5,8].

The integrated photoluminescence intensity can be expressed as

$$I_{\text{PL}} \propto G \cdot \frac{k_r}{k_r + k_{\text{nr}}}, \tag{3}$$

where G is the generation rate, k_r is the radiative recombination rate, and $k_n r$ is the non-radiative recombination rate.

Equation (3) shows that the observed PL intensity is determined by the competition between radiative and non-radiative recombination channels. Similar carrier generation and recombination mechanisms have been analyzed from photoconductivity spectra of Cd-based solid-solution films, highlighting the role of defect states and band transitions [9]. Under irradiation, defect formation leads to an increase in $k_n r$, which can be written as

$$k_{nr} = k_{nr}^{(0)} + \beta N_d, \tag{4}$$

where N_d is the concentration of radiation-induced defects.

Equation (4) indicates that the non-radiative recombination rate increases with the concentration of radiation-induced defects, which explains the quenching of photoluminescence under irradiation. Therefore, the PL intensity ratio can be written as

$$\frac{I_{\text{irr}}}{I_0} = \frac{k_r + k_{\text{nr}}^{(0)}}{k_r + k_{\text{nr}}^{(0)} + \beta N_d}. \tag{5}$$

Equation (5) provides a convenient relation for comparing the relative decrease in PL intensity before and after irradiation and can be directly related to the experimentally measured quenching ratios. For phonon-assisted transitions, the relative intensities of LO-phonon replicas can be described using the Huang–Rhys model, while the Huang–Rhys factor provides a quantitative measure of the exciton–LO-phonon coupling strength in semiconductor quantum wells [10]:

$$I_n = I_0 \exp(-S) \frac{S^n}{n!}, \tag{6}$$

where S is the Huang–Rhys factor.

Equation (6) relates the intensity distribution of the 1LO, 2LO, and 3LO replicas to the Huang–Rhys factor and thus allows estimation of the strength of exciton–phonon coupling. This model explains the presence of 1LO, 2LO, and 3LO lines observed in the spectra. More generally, Huang–Rhys theory has been extensively applied in semiconductor optical spectroscopy to interpret phonon sidebands, exciton localization effects, and the relative intensity distribution of multi-phonon replicas [11]. Furthermore, multiphoton absorption processes and intersubband transitions in III–V semiconductors provide an important contribution to the understanding of nonlinear optical effects in such systems [6,12].

To establish a direct connection between the phenomenological model and the experimental PL spectra, three measurable quantities were used in the analysis: the integrated PL intensity ratio, the irradiation-induced spectral shift, and the relative intensities of the LO-phonon replicas. First, Eq. (5) was used to interpret the experimentally observed PL quenching through the increase in the defect-assisted non-radiative recombination rate after irradiation. The measured decrease of the excitonic PL intensity by approximately two orders of magnitude indicates a substantial increase in k_{nr} compared with the initial value before irradiation. Second, the small blue and red shifts observed after electron and X-ray irradiation were interpreted as signatures of irradiation-induced changes in exciton localization and defect-related potential fluctuations. Third, Eq. (6) was used to estimate the exciton–LO-phonon coupling strength from the relative intensities of the 1LO, 2LO, and 3LO replicas through the Huang–Rhys factor. Therefore, the model was not used as an independent microscopic theory but as a quantitative phenomenological framework to correlate PL quenching, spectral shifts, and phonon-assisted emission features with radiation-induced defect formation.

EXPERIMENTAL METHOD

Low-dimensional quantum heterostructures were fabricated using state-of-the-art epitaxial techniques to ensure precise control over layer composition and thickness. ZnTe-based structures were grown by molecular beam epitaxy (MBE) employing the “Katun” system, whereas III–V heterostructures were synthesized via metal-organic chemical vapor deposition (MOCVD). Detailed growth parameters, including substrate temperature, flux ratios, and deposition rates, were optimized according to established protocols to achieve high crystalline quality and minimal structural defects.

The investigated samples are summarized in Table 1. Sample No. 1 was a ZnTe/CdZnTe-based quantum heterostructure containing three tunnel-coupled quantum wells grown by molecular beam epitaxy. Sample No. 4 was a GaAs/AlGaAs quantum-well heterostructure containing three AlGaAs/GaAs quantum wells with thicknesses of 2.5, 4.2, and 7.7 nm separated by 100 nm barriers. These samples were selected to compare the irradiation response of representative II–VI and III–V quantum heterostructures under different irradiation conditions.

Table 1. Structural parameters of the investigated quantum heterostructures.

Sample No.	Material system	Substrate	Growth method	Structure description	Quantum-well thickness	Barrier / surrounding layers	Doping concentration	Irradiation type	Measurement temperature
No. 1	ZnTe/$Cd_{0.2}Zn_{0.8}Te$	GaAs(001)	MBE using the KATUN9 system	Three tunnel-coupled $Cd_{0.2}Zn_{0.8}Te$ quantum wells embedded in ZnTe	2 nm for each QW	Barrier thickness not explicitly reported; ZnTe cap layer = 4 nm; ZnTe buffer layer = 1.5 µm	Not explicitly reported	Electron irradiation and X-ray irradiation	4.2 K
No. 4	GaAs/AlGaAs	GaAs	MOCVD	Three AlGaAs/GaAs quantum wells	2.5, 4.2, and 7.7 nm	AlGaAs barrier thickness = 100 nm	Not explicitly reported	Gamma irradiation	4.2 K and 77 K

Photoluminescence (PL) and reflectance measurements were conducted to characterize optical properties in the photon energy range of $0.6 - 3.0\ eV$ over temperatures from $4.2\ K$ to $300\ K$. Low-energy spectral components ($0.6 - 1.4\ eV$) were analyzed using a prism monochromator, while higher energies were employed with a diffraction monochromator. Photoluminescence excitation was performed using an argon-ion laser at $\lambda_{exc} = 514.53\ nm$ for ZnTe/CdZnTe quantum heterostructures. For GaAs/AlGaAs quantum wells, PL spectra were measured using excitation at $\lambda_{exc} = 632.8\ nm$. These excitation wavelengths were selected to probe excitonic emission from the quantum wells and related defect-assisted recombination channels.

For the II–VI ZnTe/CdZnTe structures, two irradiation modalities were applied: high-energy electron irradiation and X-ray photon exposure. Electron irradiation was performed using the ILU-6 pulsed accelerator, delivering electrons at $1.8\ MeV$ with a total fluence of $\Phi = 10^{16} cm^{-2}$. Pulses had a duration of 700 µs at a repetition rate of 25 Hz, with a current density of $10^{12}\ cm^{-2} \cdot s^{-1}$ per pulse. The sample temperature during irradiation did not exceed $60°C$. Energy deposition calculations indicate that the generation rate of electron-hole pairs reached $\sim 10^{23}\ cm^{-3} \cdot s^{-1}$, with the formation of radiation-induced defects via atomic displacements in the crystal lattice, estimated at $\sim 10^{17}\ cm^{-3}$.

X-ray irradiation was conducted using the RAP-150/300 source at an accelerating voltage of 100 kV, producing a continuous broad-spectrum photon flux. The dose rate was $10\ R \cdot s^{-1}$, with total exposure reaching $10^4\ R$. Absorbed energy densities in the structures were evaluated, yielding values on the order of $10^{21}\ eV \cdot cm^{-3}$, sufficient to induce significant modification of excitonic recombination channels and to generate defect states influencing photoluminescence.

For the GaAs/AlGaAs quantum-well structure, γ-irradiation was performed using a Co γ-source with a total dose of $D = 2 \times 10^9 rad$. The PL spectra were recorded before and after γ-irradiation at 77 K and 4.2 K in order to evaluate irradiation-induced changes in near-band-edge excitonic, impurity-related, and defect-related emission bands under different low-temperature measurement conditions.

All optical measurements were carried out using an automated setup integrating a low-temperature cryostat, monochromators, and photodetectors suitable for resolving excitonic emission lines, LO-phonon replicas, and impurity-related transitions. The spectral resolution of the PL measurements was determined by the monochromator configuration and was kept constant for each set of comparative measurements. Each PL spectrum was recorded under identical excitation power, temperature, and detection geometry before and after irradiation. Peak positions were extracted from the maxima of the emission bands, while integrated PL intensities were calculated after background subtraction over the same spectral interval for each band. The uncertainty in the relative intensity analysis was mainly associated with excitation-power fluctuations, detector response, and baseline correction. Repeated measurements confirmed that the main irradiation-induced trends, including PL quenching and small spectral shifts, were reproducible within the experimental uncertainty.

RESULTS

Photoluminescence of GaAs/AlGaAs Quantum Wells**.** Figure 1 presents representative low-temperature (77 K) PL spectra of sample No. 4 (Table 1), containing three AlGaAs/GaAs quantum wells, measured from the GaAs substrate side before and after γ-irradiation. The quantum well thicknesses were $L_Z = 2.5, 4.2$, and 7.7 nm, and the barrier thickness was $L_B = 100$ nm (inset of Fig. 2).

As shown in Fig. 1, the photoluminescence spectra exhibit several distinct emission bands associated with excitonic and defect-related transitions. Similar excitonic and field- or temperature-sensitive optical transitions have been analyzed in GaAs/AlGaAs multiple-quantum-well heterostructures, thereby supporting the assignment of the observed PL bands in the present study [1].

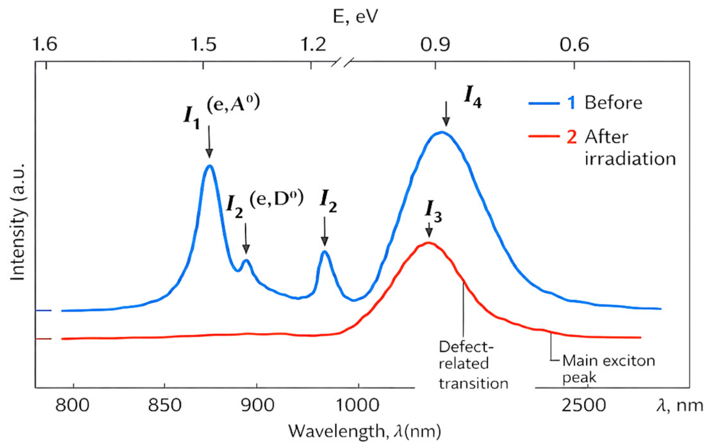

Figure 1. Typical PL spectra of the GaAs/AlGaAs quantum-well structure measured from the GaAs substrate side before (1) and after (2) gamma irradiation, D = 2×10⁹ rad, at 77 K. Excitation: λ = 632.8 nm, P = 2 W/cm².

According to the proposed model, the observed decrease in PL intensity after irradiation is associated with an increase in the non-radiative recombination rate due to radiation-induced defect formation. A comparable suppression of photoluminescence under very high electron-dose irradiation has also been reported for GaInNAs/GaAs quantum wells, further confirming the dominant role of irradiation-induced defect states in the degradation of optical response [13]. This interpretation is consistent with earlier studies of electron-irradiated GaAs-based single quantum wells, in which irradiation-induced defect states were found to alter photoluminescence intensity and spectral position through modified recombination dynamics [14]. Related irradiation-dependent changes in GaAs quantum wells have also been observed under electron-beam exposure, demonstrating that beam-induced defect modification can significantly affect luminescence intensity and recombination behavior [15].

A quantitative comparison with the proposed model was also performed. Using the relation $I_PL \propto k_r/(k_r + k_nr)$, the observed decrease in photoluminescence intensity can be attributed to a significant increase in the non-radiative recombination rate. The experimentally observed reduction of the integrated intensity ($I/I^0 \approx 10^{-2}$ for excitonic bands) is qualitatively consistent with the model prediction, indicating that radiation-induced defects dominate the recombination dynamics in the irradiated structures.

In the PL spectra of the unirradiated samples, two emission bands appear near the band edge: $I_1(\mathrm{DX}) = 1.508$ eV and $I_2(e, C) = 1.49$ eV, along with two broader bands at $I_3 = 1.38$ eV and $I_4 = 0.78$ eV. The I_1 and I_2 bands are attributed to excitons bound to donors and carbon-related electronic transitions, respectively. The weak I_3 band corresponds to donor-acceptor pair recombination, while I_4 originates from deep donor states associated with arsenic-related defects. Upon γ-irradiation ($D = 2 \times 10^9$ rad), all emission bands show a pronounced decrease in intensity (Fig. 1), consistent with the formation of non-radiative recombination centers induced by the Co γ-source. Such behavior is consistent with previous studies of photoluminescence in CdTe-based heterostructures, where defect-induced nonradiative recombination leads to strong quenching of the emission intensity [16].

For the irradiation dose considered, the ratio of post-irradiation to initial integrated intensities, I_F/I_0, was approximately 10^{-2} for the I_1 and I_2 bands, whereas $I_F/I_0 \approx 0.5$ for the I_4 band. These distinct behaviors indicate that PL quenching under irradiation cannot be attributed solely to the formation of non-radiative centers but also reflects modifications of the luminescence centers within the material, suggesting structural rearrangements of defect-related states.

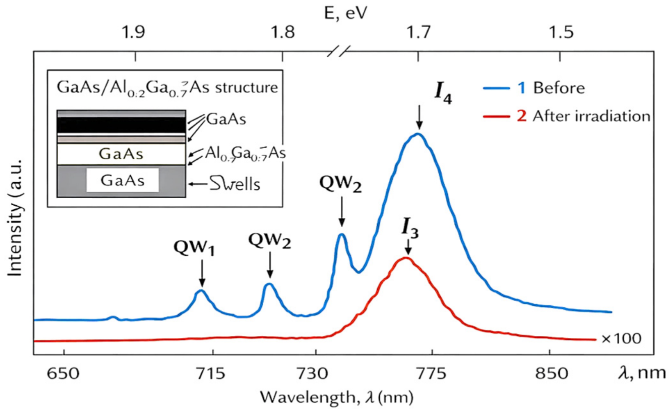

Figure 2. Low-temperature PL spectra of the GaAs/$Al_{0.2}Ga_{0.8}As$ quantum-well structure before (1) and after (2) irradiation, measured at 4.2 K. The structure contains three GaAs quantum wells with thicknesses of 2.5, 4.2, and 7.7 nm.

ZnTe/CdZnTe Quantum Wells. The PL spectra of sample No. 1 (Table 1), containing three tunnel-coupled ZnTe/$Cd_{0.2}Zn_{0.8}Te$ quantum wells, were measured with excitation $\lambda_{\text{exc}} = 0.51453\ \mu$m, corresponding to photon energies above both the ZnTe and CdZnTe band gaps as well as the electron–hole recombination energies in the wells. The low-temperature PL spectrum exhibits multiple emission features arising from the ZnTe buffer layer and the quantum wells, the latter dominating the intensity. Superimposed narrow Raman lines, shifted by multiples of the LO-phonon energy, correspond to Raman scattering of the excitation light. The non-monotonic intensity variation of Raman lines with phonon order is attributed to resonance enhancement arising from coincidences with absorption features in the buffer or quantum wells. The irradiation-induced spectral changes and LO-phonon replicas of the ZnTe/$Cd_{0.2}Zn_{0.8}Te$ quantum-well structure are shown in Fig. 3.

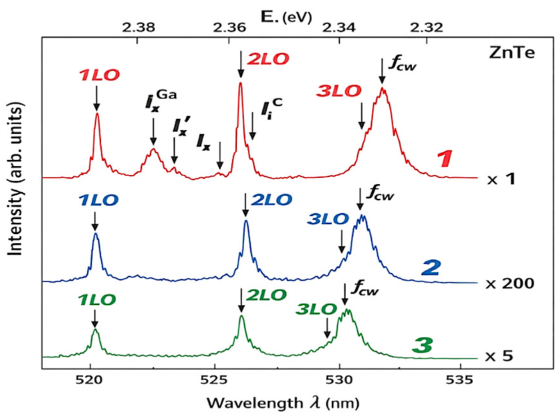

Figure 3. The spectra show pronounced 1LO, 2LO, and 3LO phonon replicas, confirming strong exciton-LO phonon coupling in the ZnTe-based structure. The changes in the relative intensities of the I_{Ga}, I_i, and f_{CW} features indicate the contribution of defect-related and excitonic recombination channels

The photoluminescence spectra of the ZnTe/CdZnTe quantum-well heterostructure exhibit distinct emission bands arising from the quantum wells (QW1 and QW2) and defect-related transitions. After irradiation, the excitonic emission intensity decreased noticeably, indicating the formation of radiation-induced defects that serve as efficient non-radiative recombination centers, degrading the optical response of the quantum wells. Similar defect-assisted suppression of optical emission has been reported in irradiated GaAs-based quantum wells [13,14], suggesting that irradiation-induced non-radiative recombination is a common feature of low-dimensional semiconductor heterostructures. Figure 3 presents the corresponding spectral changes after electron and X-ray irradiation, including the phonon-assisted emission features.

According to the model, the quenching of quantum well emission is governed by the relation $I_PL \propto k_r/(k_r + k_nr)$, where irradiation increases the defect-assisted non-radiative recombination rate. The excitonic emission at $h\nu =$ 2.3736 eV (522.4 nm) corresponds to a superposition of free exciton (IFX) and donor-bound exciton emission or exciton-polariton recombination. Lines at $h\nu = 2.37$ eV are associated with excitons bound to neutral acceptors, while a broad band at $h\nu = 2.3568$ eV is related to extended or intrinsic defect states. After both electron and X-ray irradiation (curves 2 and 3 in Fig. 3), the excitonic band intensities decrease noticeably. In the quantum well emission region, the I_{QW} band intensity also diminishes, though less markedly. Electron irradiation induced a slight blue shift ($\Delta E \approx 0.7\, meV$), whereas X-ray irradiation caused a red shift ($\Delta E \approx 0.6\, meV$). Comparable irradiation-induced energy shifts have also been reported in GaAs/AlGaAs quantum wells, where proton irradiation and post-irradiation thermal treatment modified the quantum-well transition energies [17]. Due to spectral overlap with Raman lines, potential excitonic shifts in the buffer layer were further analyzed via reflectance measurements before and after irradiation.

As shown in Fig. 3, the photoluminescence spectra of ZnTe-based quantum structures display pronounced longitudinal optical (LO) phonon replicas (1LO, 2LO, 3LO) associated with excitonic transitions. Related photoluminescence features have been observed in CdTe/ZnTe quantum nanostructures, confirming the importance of excitonic transitions in determining the spectral response of II–VI heterostructures [18]. Similar LO-phonon-assisted excitonic features have been reported in (Cd,Zn)Te-based quantum wells, where the coupling between excitons and LO phonons strongly influences the spectral structure of luminescence [19]. A closely related behavior has been reported in coupled CdTe/ZnTe quantum-well structures, where hot-exciton relaxation is governed by LO-phonon emission and strongly affects the spectral shape of optical transitions [3]. The presence of such luminescence features is consistent with previous observations in cadmium chalcogenide systems, where strong excitonic emission and spectral structure are closely related to recombination dynamics [20]. Similar photoluminescence behavior has also been reported in CdTe/ZnTe self-assembled quantum nanostructures, where excitonic emission and spectral features are strongly influenced by confinement and carrier localization effects [18]. Optical studies of ZnTe structures containing CdTe submonolayers have likewise shown that localized excitonic states strongly affect the luminescence characteristics of II–VI heterostructures [21]. The observation of multiple phonon-assisted emission lines provides clear evidence of strong exciton–phonon coupling. Resonant optical studies of II–VI quantum nanostructures have similarly demonstrated that exciton–LO phonon coupling plays a decisive role in shaping the excited-state and phonon-assisted spectral response [22]. The non-monotonic variation in the intensity of the LO replicas is attributed to resonance enhancement effects and indicates the significant role of defect states and localization phenomena in the recombination dynamics. A related sensitivity of photoluminescence behavior to localization and quantum confinement has also been reported for CdTe/ZnTe ultrathin quantum wells and size-quantized islands [23].

A quantitative estimation of the exciton–phonon coupling strength was performed using the Huang–Rhys model. Based on the relative intensities of the LO-phonon replicas (1LO, 2LO, and 3LO), the Huang–Rhys factor was estimated to be $S \approx 1 - 2$. This value indicates a moderately strong exciton–phonon interaction in ZnTe-based quantum heterostructures. The obtained result is consistent with the pronounced phonon-assisted emission features observed in the PL spectra and confirms that the coupling between excitons and LO phonons plays a significant role in the recombination processes.

QUANTITATIVE ANALYSIS OF IRRADIATION-INDUCED PL CHANGES.

To reduce the descriptive character of the analysis and to make the comparison with the phenomenological model more explicit, the main spectral parameters extracted from Figs. 1–3 are summarized in Table 2. The integrated intensity ratio $\frac{I_F}{I_0}$ was used as the primary measure of PL quenching. Since all spectra were recorded under identical excitation power, temperature, and detection geometry, a decrease in $\frac{I_F}{I_0}$ can be directly associated with an increased contribution of defect-assisted non-radiative recombination. In the limiting case in which the radiative recombination rate and generation rate remain approximately unchanged, an effective non-radiative contribution may be estimated as $\eta_{\text{eff}} = \left(\frac{I_0}{I_F}\right) - 1$. This parameter is not an absolute defect density; rather, it is a comparative measure of irradiation-induced optical degradation in the investigated heterostructures.

Table 2. Quantitative indicators of irradiation-induced photoluminescence modifications in the investigated quantum heterostructures.

Material system	Irradiation type	Observed parameter	Quantitative indicator	Physical implication
GaAs/AlGaAs quantum wells	γ-irradiation	Near-band-edge excitonic and impurity-related emission (I_1, I_2)	$\frac{I_F}{I_0} \approx 10^{-2}$	Strong suppression of radiative recombination due to the formation of radiation-induced non-radiative centers
GaAs/AlGaAs quantum wells	γ-irradiation	Deep defect-related emission (I_4)	$\frac{I_F}{I_0} \approx 0.5$	Deep-level emission is less sensitive to irradiation than shallow excitonic channels
ZnTe/CdZnTe quantum wells	Electron irradiation	Quantum-well excitonic transition	$\Delta E \approx +0.7\, meV$	Slight blue shift associated with irradiation-induced modification of exciton localization and local potential profile
ZnTe/CdZnTe quantum wells	X-ray irradiation	Quantum-well excitonic transition	$\Delta E \approx -0.6\, meV$	Small red shift indicating enhanced defect-related localization and potential fluctuations
ZnTe/CdZnTe quantum wells	Electron and X-ray irradiation	LO-phonon-assisted emission (1LO, 2LO, 3LO)	Huang–Rhys factor $S \approx 1 - 2$	Moderately strong exciton–LO-phonon coupling contributing to phonon-assisted recombination
All investigated structures	All irradiation conditions	Overall PL response	Intensity quenching and spectral redistribution	Radiation-induced defects alter the balance between radiative and non-radiative recombination channels

The quantitative comparison shows that the most pronounced effect of irradiation is the suppression of shallow excitonic and impurity-related emission in the GaAs/AlGaAs structure. The approximately two-orders-of-magnitude decrease of the I_1 and I_2 bands corresponds to a strong increase in the effective non-radiative contribution, whereas the I_4 band retains nearly half of its initial integrated intensity. This behavior suggests that different luminescence centers have different radiation sensitivities and that PL quenching is accompanied by a redistribution of recombination channels.

For the ZnTe/CdZnTe quantum wells, the opposite signs of the spectral shifts after electron and X-ray irradiation are small but reproducible. Therefore, they should not be interpreted as large changes in the band gap. Instead, they are more consistently understood as changes in the ensemble of localized excitons contributing to the PL maximum. A rigorous linewidth decomposition was not performed because the spectra contain partially overlapping excitonic bands, Raman lines, and LO-phonon replicas. For this reason, the present analysis uses integrated intensities, peak shifts, and relative phonon-replica intensities as the most reliable comparative parameters.

DISCUSSION

The observed PL intensity reductions and spectral shifts indicated that γ-ray, X-ray, and electron irradiation modified both the recombination dynamics and the local energy landscape of excitonic and impurity-related states. This interpretation is consistent with theoretical descriptions of absorption and carrier relaxation processes in semiconductors, where radiation-induced defects can strongly affect recombination channels [5,8]. The different responses of the emission bands suggest that shallow donor- and acceptor-bound excitons are more sensitive to irradiation than deep defect-related states, leading to selective quenching of radiative channels. At the same time, the observed blue and red shifts in the quantum-well emission bands suggest irradiation-induced modifications of exciton localization and defect-related potential fluctuations. The presence of LO-phonon replicas with modulated intensities further confirms the role of exciton–phonon coupling and resonance effects in the recombination dynamics. Overall, the PL response provides a sensitive probe of irradiation-induced defect formation, exciton dynamics, and phonon-assisted processes in semiconductor quantum heterostructures.

The observed trends are qualitatively consistent with the proposed phenomenological model. The obtained results are also consistent with theoretical studies of interband and multiphoton absorption processes, which emphasize the role of band mixing and nonlinear optical effects in semiconductor heterostructures [6,12].

From a microscopic point of view, the decrease in PL intensity can be explained by the formation of vacancies, interstitials, antisite defects, and defect complexes that introduce additional electronic states inside the band gap. These centers provide Shockley–Read–Hall-type non-radiative pathways and reduce the probability of radiative exciton recombination. Shallow donor-bound and acceptor-bound excitons are especially sensitive to such perturbations because their recombination depends strongly on the local potential landscape and on the overlap between electron and hole wave functions.

The distinction between electron irradiation and photon irradiation is also important. High-energy electrons can transfer momentum directly to lattice atoms, thereby producing displacement damage more efficiently, whereas X-ray and gamma-ray photons primarily produce ionization, secondary carriers, charge trapping, and defect charging, with atomic displacement occurring mainly through secondary processes. This difference provides a plausible explanation for the different spectral responses observed in the ZnTe/CdZnTe structures. The blue shift after electron irradiation may be related to preferential quenching of lower-energy localized states or to slight radiation-induced modification of the well/barrier potential profile. In contrast, the red shift after X-ray irradiation may reflect enhanced exciton localization in defect-related potential minima or local electric-field-induced band bending.

The observed energy shifts of approximately 0.6–0.7 meV are small relative to the transition energies but are important because they occur together with substantial PL quenching. This indicates that irradiation affects not only the total recombination efficiency but also the distribution of radiative states that contribute to the PL maximum. Thus, the shifts should be treated as signatures of a modified localized-exciton ensemble rather than as direct evidence of a large change in the fundamental band gap.

The LO-phonon replicas provide additional information on the recombination process. The estimated Huang–Rhys factor $S \approx 1 - 2$ indicates moderately strong exciton–LO-phonon coupling. After irradiation, defect-induced localization can enhance the interaction of excitons with lattice vibrations and redistribute intensity between the zero-phonon and phonon-assisted channels. However, because the LO replicas partly overlap with Raman features, the extracted S value should be regarded as a semi-quantitative estimate rather than as a uniquely fitted microscopic parameter.

It should be emphasized that the defect concentration discussed in this work is evaluated indirectly from PL quenching and spectral redistribution. Direct determination of absolute defect densities would require complementary techniques such as time-resolved PL, deep-level transient spectroscopy, electron paramagnetic resonance, or high-resolution structural analysis. Nevertheless, the present steady-state PL approach provides a useful comparative framework for assessing radiation-induced optical degradation in III–V and II–VI quantum heterostructures.

CONCLUSIONS

The effects of high-energy γ-ray, X-ray, and electron irradiation on the photoluminescence (PL) response of III–V and II–VI quantum heterostructures were investigated using low-temperature PL spectroscopy. For the GaAs/AlGaAs quantum-well structure, γ-irradiation caused a strong reduction in the intensities of near-band-edge excitonic and defect-related emission bands. The integrated intensity ratio decreased to approximately $I_F/I_0 \approx 10^{-2}$ for the I_1 and I_2 bands, whereas the deeper defect-related I_4 band retained about half of its initial intensity, i.e., $I_F/I_0 \approx 0.5$. This difference indicates that shallow donor- and impurity-related radiative channels are more sensitive to irradiation-induced non-radiative recombination than deeper defect-related states.

For the ZnTe/CdZnTe quantum-well structures, electron and X-ray irradiation also modified the excitonic emission and phonon-assisted spectral features. Electron irradiation induced a slight blue shift of the quantum-well emission, whereas X-ray irradiation caused a small red shift, with the spectral shifts remaining in the range of $\Delta E \approx 0.6 - 0.7\ meV$. These opposite spectral shifts suggest that different irradiation conditions can modify exciton localization and defect-related potential fluctuations in different ways. The observation of 1LO, 2LO, and 3LO phonon replicas, together with the estimated Huang–Rhys factor of $S \approx 1 - 2$, confirms that exciton–LO-phonon coupling contributes significantly to the luminescence response of the ZnTe/CdZnTe structures.

Overall, the results show that irradiation affects both the intensity and energy position of PL bands through the formation of radiation-induced defects and the redistribution of radiative and non-radiative recombination channels. The GaAs/AlGaAs results mainly demonstrate the effect of γ-irradiation on III–V quantum wells, whereas the ZnTe/CdZnTe results clarify the influence of electron and X-ray irradiation on II–VI quantum wells. Therefore, the present work provides a comparative PL-based assessment of irradiation-induced modifications in representative III–V and II–VI quantum heterostructures. These findings may be useful for evaluating the radiation tolerance of low-dimensional semiconductor structures intended for optoelectronic applications in radiation environments.

The main limitation of the present study is that the quantitative defect analysis is based on steady-state PL parameters rather than on direct microscopic defect spectroscopy. Therefore, the reported intensity ratios, spectral shifts, and Huang–Rhys factor should be viewed as comparative indicators of irradiation sensitivity. Future studies combining PL with time-resolved spectroscopy and independent defect-characterization techniques would allow more rigorous extraction of recombination lifetimes, linewidth broadening, and absolute defect densities.

Acknowledgments

The authors sincerely thank **Prof. Rasulov Rustam Yavkachovich, Professor of the Department of Physics at Fergana State University**, for his valuable scientific guidance, helpful suggestions, and constructive discussions.

Conflict of Interest

The authors declare no conflict of interest.

ORCID

Mardonbek X. Nasirov, https://orcid.org/0000-0002-6811-072X;
Dilmuhammad X. Tolaboyev, https://orcid.org/0000-0001-6248-845X;
Tohirjon I. Raxmonov, https://orcid.org/0000-0002-6080-6159;
Husanboy M. Sulaymonov, https://orcid.org/0000-0003-0790-1584;
Sherzod Sh. Abdullaev, https://orcid.org/0009-0007-9768-5008;
Abdusattor O. Umarov, https://orcid.org/0000-0003-1624-7705;
Ixtiyor M. Tursunov, https://orcid.org/0009-0009-0864-2204

REFERENCES

[1] Türkoğlu, A., Ergün, Y., & Ungan, F. "Investigation of the electro-optical characteristics of GaAs/AlGaAs multiple quantum well grown by metal-organic vapor phase epitaxy," Journal of Molecular Structure, **1279**, 134202 (2023). https://doi.org/10.1016/j.molstruc.2022.134202

[2] Akhmadaliev, B. Z., Yuldashev, N. K., & Yulchiev, I. I. "Surface-radiative modes and longitudinal excitons in the spectra of exciton-polariton luminescence," Optics and Spectroscopy, **125**, 343–352 (2018). https://doi.org/10.1134/S0030400X18090023

[3] Liu, X.-Y., Singh, C. N., Kennedy, E. R., Huang, S., Fluckey, S. P., Matthews, C., & Uberuaga, B. P. "Review of radiation-induced defects in GaAs," Journal of Applied Physics, **138**(7), 070701 (2025). https://doi.org/10.1063/5.0279267

[4] Mirzaev, V. T., Akhmadaliyev, B. J., Yulchiev, I. I., Madraximov, M. M., & Rakhmonov, T. I. "Temperature and infrared quenching of equilibrium conductivity in $CdSe_xS_{1-x}$ film," East European Journal of Physics, (2), 247–251 (2025). https://doi.org/10.26565/2312-4334-2025-2-29

[5] Rasulov, R. Y., Rasulov, V. R., Kodirov, N. U., Nasirov, M. K., & Eshboltaev, I. M. "Theoretical analysis of interband single-photon light absorption in semiconductors: Effects of valence-conduction band mixing and temperature-dependent bandgap," East European Journal of Physics, (2), 179–187 (2025). https://doi.org/10.26565/2312-4334-2025-2-18

[6] Rasulov, R. Y., Rasulov, V. R., Kasimov, F. U., Nasirov, M. K., Farmanova, I. E., & Tursinbaev, A. Z. "On the theory of two-photon intersubband absorption and linear-circular dichroism in semiconductors of the III–V type," East European Journal of Physics, (2), 188–199 (2025). https://doi.org/10.26565/2312-4334-2025-2-19

[7] Agekyan, V. F., Budkin, G., Chukeev, M., Filosofov, N., Karczewski, G., Serov, A., & Reznitsky, A. "Hot exciton relaxation in coupled ultra-thin CdTe/ZnTe quantum well structures," Journal of Luminescence, **230**, 117762 (2021). https://doi.org/10.1016/j.jlumin.2020.117762

[8] Rasulov, R. Y., Rasulov, V. R., Kasimov, F. U., Nasirov, M. K., & Muminov, I. A. "On the theory of the intraband mechanism of single-photon absorption in semiconductors, taking into account the effect of coherent saturation," East European Journal of Physics, (2), 441–451 (2025). https://doi.org/10.26565/2312-4334-2025-2-55

[9] Akhmadaliyev, B., Rakhmonov, T., Sulaymonov, K., & Nurmatov, O. "Photoconductivity spectra of thin solid solution films $CdSe_xS_{1-x}$," E3S Web of Conferences, **583**, 04002 (2024). https://doi.org/10.1051/e3sconf/202458304002
[10] Huo, B., Zhang, H., Jiang, Y., Chen, Q., & Wang, Z. M. "The Huang–Rhys factor and the strength of exciton–LO phonon coupling in semiconductor quantum wells," Materials Today: Proceedings, (2007). https://doi.org/10.1016/S1369-8001(08)00021-8
[11] Zhang, Y. "Applications of Huang–Rhys theory in semiconductor optical spectroscopy," Journal of Semiconductors, **40**(9), 091102 (2019). https://doi.org/10.1088/1674-4926/40/9/091102
[12] Rasulov, R. Y., Rasulov, V. R., Kasimov, F. U., Nasirov, M. K., Farmanova, I. E., & Tursinbaev, A. Z. "On the theory of interband two-photon absorption of light in semiconductors accounting admixtures to the states of the conduction band and valence states, the Rabi effect," East European Journal of Physics, (2), 200–205 (2025). https://doi.org/10.26565/2312-4334-2025-2-20
[13] Pavelescu, E. M., Bălţăţeanu, N., Spânulescu, S. I., & Arola, E. "Very high dose electron irradiation effects on photoluminescence from GaInNAs/GaAs quantum wells grown by molecular beam epitaxy," Optical Materials, **64**, 361–365 (2017). https://doi.org/10.1016/j.optmat.2016.12.007
[14] Sailai, M., Aierken, A., Li, Q., Heini, M., Zhao, X., Mo, J., Gao, J., *et al.*, "Effects of 1-MeV electron irradiation on the photoluminescence of GaInNAs/GaAs single quantum well structure," Semiconductors, **54**, 554–557 (2020). https://doi.org/10.1134/S1063782620050103
[15] Murata, T., Ohno, Y., Kishimoto, S., & Mizutani, T. "Photoluminescence intensity enhancement by electron beam irradiation into GaAs quantum wells," Solid-State Electronics, **43**(1), 147–152 (1999). https://doi.org/10.1016/S0038-1101(98)00197-X
[16] Polvonov, B. Z., Gafurov, Y. I., Otajonov, U. A., Nasirov, M. X., & Zaylobiddinov, B. B. "The specificity of photoluminescence in n-CdS/p-CdTe semiconductor heterostructures," International Journal of Mathematics and Physics, **13**(2), (2022). https://doi.org/10.26577/ijmph.2022.v13.i2.02
[17] Tan, H. H., Williams, J. S., Jagadish, C., Burke, P. T., & Gal, M. "Large energy shifts in GaAs–AlGaAs quantum wells by proton irradiation-induced intermixing," Applied Physics Letters, **68**(17), 2401–2403 (1996). https://doi.org/10.1063/1.116147
[18] Romčević, N., Romčević, M., Kostić, R., Stojanović, D., Milutinović, A., Trajić, J., Karczewski, G., & Galazka, R. "Photoluminescence spectroscopy of CdTe/ZnTe self-assembled quantum dots," International Journal of Photoenergy, 2009, 358790 (2009). https://doi.org/10.1155/2009/358790
[19] Stanley, R. P., Doran, J. P., Hegarty, J., & Feldman, R. D. "LO-phonons and excitons in (Cd,Zn)Te based quantum wells," Physica B: Condensed Matter, **191**(1–2), 71–82 (1993). https://doi.org/10.1016/0921-4526(93)90179-A
[20] Ayibzhanov, M., Mamatov, O., Mirzaev, V., & Tuychibaev, B. "Luminescence spectrum of cadmium chalcogenide photovoltaic film structures and their power enhancement," E3S Web of Conferences, **583**, 04003 (2024). https://doi.org/10.1051/e3sconf/202458304003
[21] Agekyan, V. F., Serov, A. Y., Filosofov, N. G., Shtrom, I. V., & Karczewski, G. "Optical properties of zinc telluride with cadmium telluride submonolayers," Physics of the Solid State, **58**(10), 2109–2112 (2016). https://doi.org/10.1134/S1063783416100036
[22] Nguyen, T. A., Mackowski, S., Jackson, H. E., Smith, L. M., Wrobel, J., Fronc, K., Karczewski, G., *et al.*, "Resonant spectroscopy of II–VI self-assembled quantum dots: Excited states and exciton–longitudinal optical phonon coupling," Physical Review B, **70**, 125306 (2004). https://doi.org/10.1103/PhysRevB.70.125306
[23] Zaitsev, V. V., Bagaev, V. S., & Onishchenko, E. E. "Specific features in the temperature dependence of photoluminescence from CdTe/ZnTe size-quantized islands and ultrathin quantum wells," Physics of the Solid State, **41**, 647–653 (1999). https://doi.org/10.1134/1.1130842

РАДІАЦІЙНО-ІНДУКОВАНА МОДИФІКАЦІЯ КВАНТОВИХ ГЕТЕРОСТРУКТУР III–V ТА II–VI ПІД ВПЛИВОМ ВИСОКОЕНЕРГЕТИЧНОГО РЕНТГЕНІВСЬКОГО, ГАММА- ТА ЕЛЕКТРОННОГО ОПРОМІНЕННЯ

Мардонбек Х. Насіров[1,2], Ділмухаммад Х. Толабоєв[1], Тохірджон І. Рахмонов[1], Хусанбой М. Сулаймонов[1], Шерзод Ш. Абдуллаєв[1], Абдусаттор О. Умаров[1], Ікстійор М. Турсунов[1]
[1]*Ферганський державний технічний університет, Фергана, Узбекистан*
[2]*Ферганський державний університет, Фергана, Узбекистан*

Низькорозмірні квантові гетероструктури III–V та II–VI є важливими активними середовищами для оптоелектронних пристроїв, що працюють в умовах радіаційного впливу. У цій роботі досліджено вплив високоенергетичного рентгенівського, гамма- та електронного опромінення на екситонну рекомбінацію та екситон-фононну взаємодію в квантових гетероструктурах GaAs/AlGaAs і ZnTe/CdZnTe за допомогою низькотемпературної фотолюмінесцентної спектроскопії. Спектри показали виражені смуги екситонного випромінювання, що супроводжуються репліками поздовжніх оптичних фононів, що свідчить про фононно-асистовані процеси рекомбінації. Після опромінення спостерігалося значне зменшення інтенсивності фотолюмінесценції, що пов'язано з утворенням радіаційно-індукованих центрів безвипромінювальної рекомбінації. У структурах ZnTe/CdZnTe електронне опромінення спричиняло невеликий синій зсув (приблизно 0,7 меВ) випромінювання квантової ями, тоді як рентгенівське опромінення приводило до малого червоного зсуву (приблизно 0,6 меВ), що вказує на залежну від типу опромінення модифікацію локалізації екситонів і дефектно-зумовлених флуктуацій потенціалу. Виконано напівкількісний аналіз на основі відношень інтегральної інтенсивності фотолюмінесценції, ефективного параметра безвипромінювальної рекомбінації та фактора Хуанга–Ріса $S \approx 1-2$, що дозволило пов'язати гасіння фотолюмінесценції, спектральні зсуви та репліки LO-фононів з утворенням радіаційно-індукованих дефектів. Відносні зміни екситонних, домішкових і фононно-асистованих смуг випромінювання вказують на перерозподіл радіаційних і безвипромінювальних каналів рекомбінації після опромінення. Феноменологічна інтерпретація, заснована на радіаційних і безвипромінювальних швидкостях рекомбінації та описі реплік LO-фононів за моделлю Хуанга–Ріса, була використана для пояснення спостережуваних спектральних змін. Отримані результати забезпечують порівняльну експериментальну оцінку радіаційно-індукованих модифікацій у квантових гетероструктурах III–V та II–VI і можуть бути корисними для оцінювання радіаційної стійкості напівпровідникових оптоелектронних структур.

Ключові слова: *радіаційно-індуковані дефекти; квантові гетероструктури; фотолюмінесцентна спектроскопія; екситон-фононна взаємодія; репліки LO-фононів; безвипромінювальна рекомбінація; квантові ями GaAs/AlGaAs; квантові ями ZnTe/CdZnTe*